



Int. J. New. Chem., 2022, Vol. 9, Issue 4, pp. 393-404.

International Journal of New Chemistry

Published online 2022 in <http://www.ijnc.ir/>

Open Access

Print ISSN: 2645-7236

Online ISSN: 2383-188x



Original Research Article

A DFT Investigation on Fullerene (C₂₀) Interaction with Nalidixic Acid

Saeid Abrahi Vahed¹, Fatemeh Hemmati Tirabadi^{2,3,*}

¹Young Researchers and Elite Club, Tehran Medical sciences, Islamic Azad university, Tehran, Iran

^{2,*}Department of Chemistry, Yadegar-e-Imam Khomeini (RAH) Shahre Rey Branch, Islamic Azad University, Tehran, Iran

^{3,*}Research Center for New Technologies in Chemistry and Related Sciences, Yadegar-e-Imam Khomeini (RAH) Shahre Rey Branch, Islamic Azad University, Tehran, Iran

Received: 2022-11-01

Accepted: 2022-12-15

Published: 2022-12-22

ABSTRACT

The removal and detection of nalidixic acid (NA) as an emerging environmental contaminant and a medicine are of great importance. In this respect, the performance of fullerene (C₂₀) as a sensing material and an adsorbent for NA was investigated by infrared-red (IR), frontier molecular orbital (FMO), and natural bond orbital (NBO) computations. The calculated adsorption energies, Gibbs free energy changes, enthalpy changes, and thermodynamic constants showed that NA interaction with C₂₀ was experimentally feasible, exothermic, and spontaneous. The NBO results indicated that NA interaction with C₂₀ was physisorption and no bond was created among the adsorbent and adsorbate. Moreover, findings on the effect of the temperature indicated that the adsorption process was more favorable at lower temperatures. The computed bandgap values showed that when NA was adsorbed on the surface of C₂₀, the bandgap of fullerene experienced a sharp increase (+298.462%) from 1.950 to 7.770 (eV). Hence, this nanostructure is a suitable sensing material for the development of novel electrochemical sensors for the determination of NA.

Keywords: Nalidixic acid, Fullerene, Density Functional Theory, Adsorption, Sensor

Introduction

*Corresponding Author: Tel.: +98 9197387925
E-mail: fatemehemmati.t@yahoo.com

In the last few years, pharmaceuticals have caused a growing concern due to their presence in environmental samples. Among these compounds, it should be highlighted that, the antibiotics which are used in large quantities for several decades as human infection medicine, veterinary medicine, and husbandry growth promoters. Due to incomplete metabolization of these compounds in human and animal body, a portion of administered antibiotic is excreted as the parent compound or as metabolites via urine and feces. As a result of the agricultural application of manure and sewage sludge containing unmetabolized drugs, wastewater irrigation, and the disposal of domestic and hospital waste, they are eventually released into soils, sediments, and aquatic environments through different pathways[1–3]. Nalidixic acid (NA) (1-ethyl-1,4-dihydro-7-methyl-4-oxo-1,8-naphthyridine-3 carboxylic acid), as shown in Figure 1, is the first synthetic quinolone antibiotic that was introduced in therapy in the 1960s [4]. NA is effective against both gram-positive and gram-negative microbes. It acts as a bacteriostatic agent in lower concentrations, but can be bactericidal at higher concentrations. Nalidixic acid has been selected in the present study because of its presence in hospital wastes, wastewater treatment plants effluents, environmental waters and soils [5-7]. It has serious effects on human health, such as chronic toxicity and carcinogenicity effect [8]. Various methods for removing nalidixic acid from aqueous solutions were used, including an embedded MBR-ozonation scheme [9], powdered activated carbon [10], adsorption on to anion-exchange and neutral polymers [11] and UV and UV/H₂O₂ processes [12]. Adsorption, as a simple and relatively economic method, is widely utilized in the removal of pollutants. On the other hand, fullerene (C₂₀, Figure 1) is the smallest nanomaterial with a dodecahedral cage structure [13-18]. The structure of this fullerene is highly curved and it is composed of pentagonal rings. C₂₀ has unique traits that make it an eminent sensing material like high conductance, great surface area/ volume ratio and excellent reactivity [19-31]. In this respect, the goal of this study is to evaluate the sensing performance of C₂₀ for electrochemical detection and removal of NA by density functional theory simulations.

Computational Details

Software versions GaussView 6 and Nanotube modeler 1.3.0.3 were used to design the structures of C₂₀, NA, and their complexes [18-19]. Each of the structures that were designed first underwent geometric optimization. After that, computations for IR, FMO, and NBO were performed on designed structures. The density functional theory method was used throughout the computations by Gaussian 16 software at the B3LYP/6-31G (d) level of theory [20]. This level was selected since the findings obtained from earlier studies were acceptable and were consistent with experimental results. The densities of states (DOS) spectrums were obtained using the GaussSum 3.0 software [21]. All computations were performed in the vacuum between 298 and 398 K at intervals of 10°.

The following processes were investigated [22]:



Adsorption energy values (E_{ad}) and thermodynamic parameters, such as thermodynamic equilibrium constant (K_{th}), Gibbs free energy changes (ΔG_{ad}), entropy changes (ΔS_{ad}), and adsorption enthalpy changes (ΔH_{ad}), were calculated using equations 2–6 [23-25].

$$E_{\text{ad}} = \left(E_{(\text{Complex})} - (E_{(\text{NA})} + E_{(\text{Adsorbent})} + E_{(\text{BSSE})}) \right) \quad (2)$$

$$\Delta H_{\text{ad}} = \left(H_{(\text{Complex})} - (H_{(\text{NA})} + H_{(\text{Adsorbent})}) \right) \quad (3)$$

$$\Delta G_{\text{ad}} = \left(G_{(\text{Complex})} - (G_{(\text{NA})} + G_{(\text{Adsorbent})}) \right) \quad (4)$$

$$\Delta S_{\text{ad}} = \left(S_{(\text{Complex})} - (S_{(\text{NA})} + S_{(\text{Adsorbent})}) \right) \quad (5)$$

$$K_{\text{th}} = \exp\left(-\frac{\Delta G_{\text{ad}}}{RT}\right) \quad (6)$$

In the equations above, E stands for the total electronic energy for every structure, E_{BSSE} stands for the basis set superposition correction, and H represents the total energy of the evaluated materials plus the thermal correction of enthalpy. For each structure under study, the G denotes

the total energy plus the thermal correction of the Gibbs free energy [22]. R represents the constant of the ideal gas, S is the thermal correction entropy for the studied structures, and T stands for temperature [26-28].

Equations 7–12 were used to calculate the bandgap (E_g), chemical hardness (η), chemical potential (μ), maximum charge capacity (ΔN_{\max}), and the electrophilicity (ω) of frontier molecular orbitals [29-31].

$$E_g = E_{\text{LUMO}} - E_{\text{HOMO}} \quad (7)$$

$$\% \Delta E_g = \frac{E_{g2} - E_{g1}}{E_{g1}} \times 100 \quad (8)$$

$$\eta = (E_{\text{LUMO}} - E_{\text{HOMO}}) / 2 \quad (9)$$

$$\mu = (E_{\text{LUMO}} + E_{\text{HOMO}}) / 2 \quad (10)$$

$$\omega = \mu^2 / 2\eta \quad (11)$$

$$\Delta N_{\max} = -\mu / \eta \quad (12)$$

E_{LUMO} , in the equations above, is the energy of the lowest unoccupied molecular orbital, and E_{HOMO} is the energy of the highest occupied molecular orbital. The bandgaps of the Nano-adsorbent and NA-Adsorbent complexes are shown as E_{g1} and E_{g2} , respectively [29].

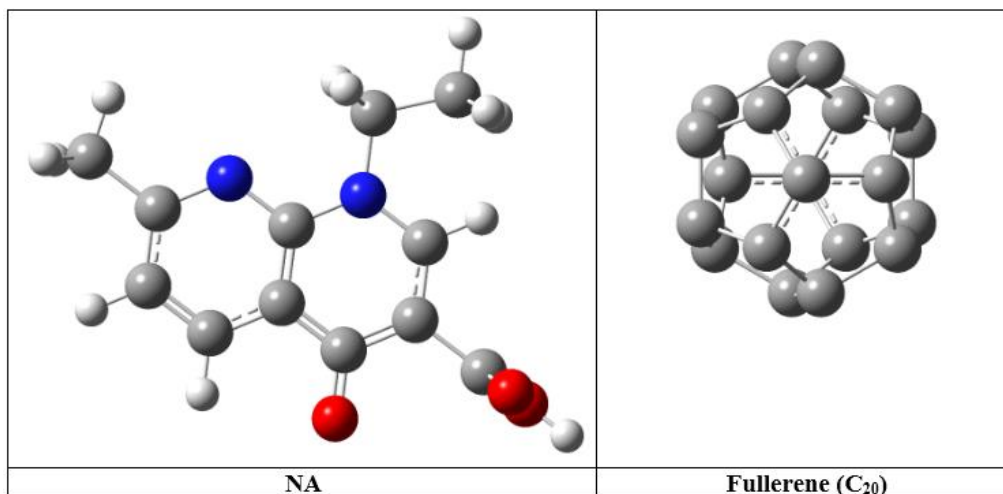


Figure 1. The optimized structures of fullerene (C₂₀) and NA (oxygen: red, nitrogen: blue, carbon: gray, hydrogen: white)

Results and Discussion

NA interaction with C₂₀ was scrutinized at three various configurations to achieve the conformer with the highest stability. The initial structures and the optimized versions of those are presented in Figure 2. It demonstrates that the carbonyl and carboxylic acid functional groups of NA was inserted near the C₂₀ at A-Conformer. In B-Conformer, the adsorbate was located near the adsorbent towards its aliphatic substitutions, and in C-Conformer, the NA molecule was placed adjacent to C₂₀ towards its naphthyridine ring. As seen from the provided optimized structures in Figure 2, after geometrical optimizations, the NA molecule only come closer to fullerene, and no tangible structural deformations occurred in the adsorbate and adsorbent molecules. Both findings indicate that NA interaction with C₂₀ is relatively weak. Table 1 displays the determined adsorption and total electronic energies. As shown, all of the scrutinized conformers have negative adsorption energy values, which shows experimentally possibility of the adsorption of NA on the C₂₀ surface at all of the studied configurations. Also, according to this table, fullerene nanocage is an effective adsorbent for NA removal [25-30]. The optimized structures were also subjected to IR computations, and Table 1 provides the highest and lowest obtained IR frequencies. According to this table, all the structures that were investigated are true

local minimums since there is obviously no negative vibrational frequency. Dipole moment values were also computed. These values revealed that with NA adsorption on the surface of fullerene, the dipole moment increases remarkably, indicating that with the formation of NA-C₂₀ complexes, their reactivity becomes higher than pure NA. The optimized structures were also subjected to NBO computations to learn more about the adsorption mechanism. The outcomes demonstrated that the formation of a chemical bond between NA and nanostructure was prevented in all the examined conformers [26-34].

Table1. The values of total electronic energy, adsorption energy, zero-point energy (ZPE), the maximum and minimum IR frequencies and dipole moment for NA, C₂₀ and their complexes

	Total electronic energy (a.u)	Adsorption energy (kJ/mol)	ZPE (kJ/mol)	ν_{\min} (cm ⁻¹)	ν_{\max} (cm ⁻¹)	Dipole Moment (Debye)
NA	-784.860	---	692.680	9.707	4093.279	0.880
C ₂₀	-747.196	---	325.260	261.392	1690.640	0.000
A-Conformer	-1532.088	-84.150	1040.350	3.682	4241.622	4.250
B-Conformer	-1532.100	-115.656	1040.510	1.800	4242.268	5.310
C-Conformer	-1532.091	-92.026	1040.630	1.948	4242.409	4.660

The thermodynamic parameters calculated for the process of NA adsorption are shown in Figure 3 as a function of temperature, including ΔH_{ad} , ΔG_{ad} , ΔS_{ad} , and the logarithm of K_{th} . Clearly, all the conformers under investigation have negative ΔH_{ad} values. These values show the exothermic nature of the adsorption process. The NA adsorption process is spontaneous, two-sided and equilibrium as shown by the low quantities of thermodynamic constants and the negative amounts for ΔG_{ad} . The drop-in chaos is shown by the negative values of ΔS_{ad} in the IQ

adsorption process. Also, these negative values exhibit that the entropy of the NA interaction with C_{20} is unsuitable. According to the results of the investigation into how temperature affects all of the thermodynamic parameters, the temperature fluctuations did not significantly impact the adsorption process, and NA interaction with fullerene is somewhat more favorable at lower temperatures [25-28]. The difference between the HOMO and LUMO orbital energies is the band gap, which is inversely related to the electrical conductivity of materials. The electrical conductivity of materials with a narrow band gap is higher than the materials with a wide one [29]. Therefore, to assess the efficiency of C_{20} as an electrochemical sensor for measuring NA, this parameter was computed for the each of individual structures. According to the data presented in Table 2, the E_g of fullerene nanocage is 1.950 (eV). When NA is adsorbed on its surface, this parameter tangibly increases to 7.770, 7.740, and 7.730 (eV), respectively, for A, B, and C conformers. It appears C_{20} can be used as an appropriate material for developing electrochemical sensors for NA detection, as this nanostructure bandgap variation is only about 298% for all three investigated configurations [30]. Equations 9–12 were used to calculate the electrophilicity, chemical hardness, maximum transferred charge capacity, and chemical potential. Table 2 shows the results. It reveals that the NA chemical hardness for the A, B, and C conformers decreases from 5.443 (eV) to 3.885, 3.870, and 3.865 (eV), respectively, when NA is adsorbed on the surface of fullerene. As a result, NA- C_{20} complexes are softer and more reactive than pristine NA that does not contain a nano adsorbent [28]. All investigated structures have a negative measured chemical potential, suggesting that they all have thermodynamic stability [29]. Following its interaction with C_{20} , NA becomes more electrophilic and has a higher maximum transferred charge capacity, indicating that NA- C_{20} complexes have higher electrophilicity and, compared to pristine NA, are more likely to absorb electrons [24-31].

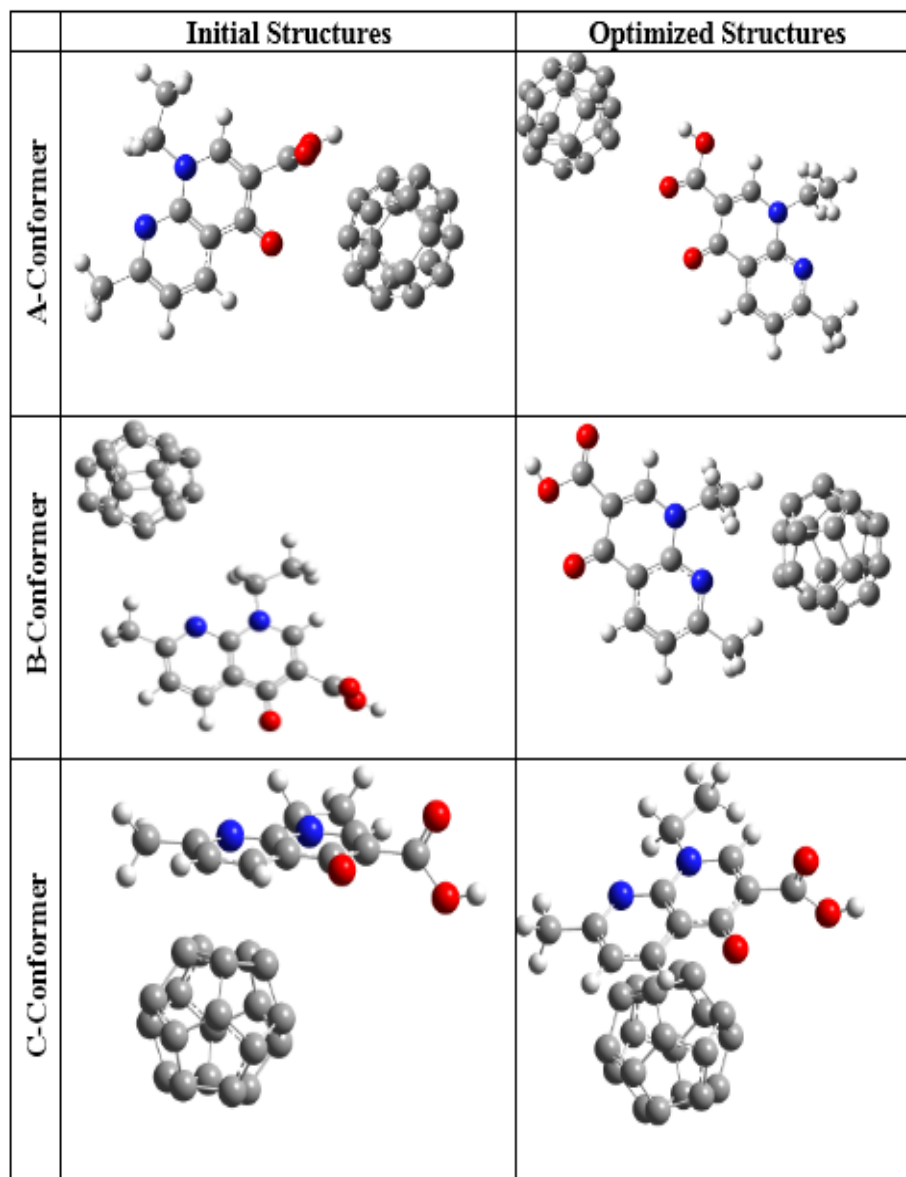


Figure 2. Initial and optimized structures of NA-C₂₀ complexes (oxygen: red, nitrogen: blue, carbon: gray, hydrogen: white)

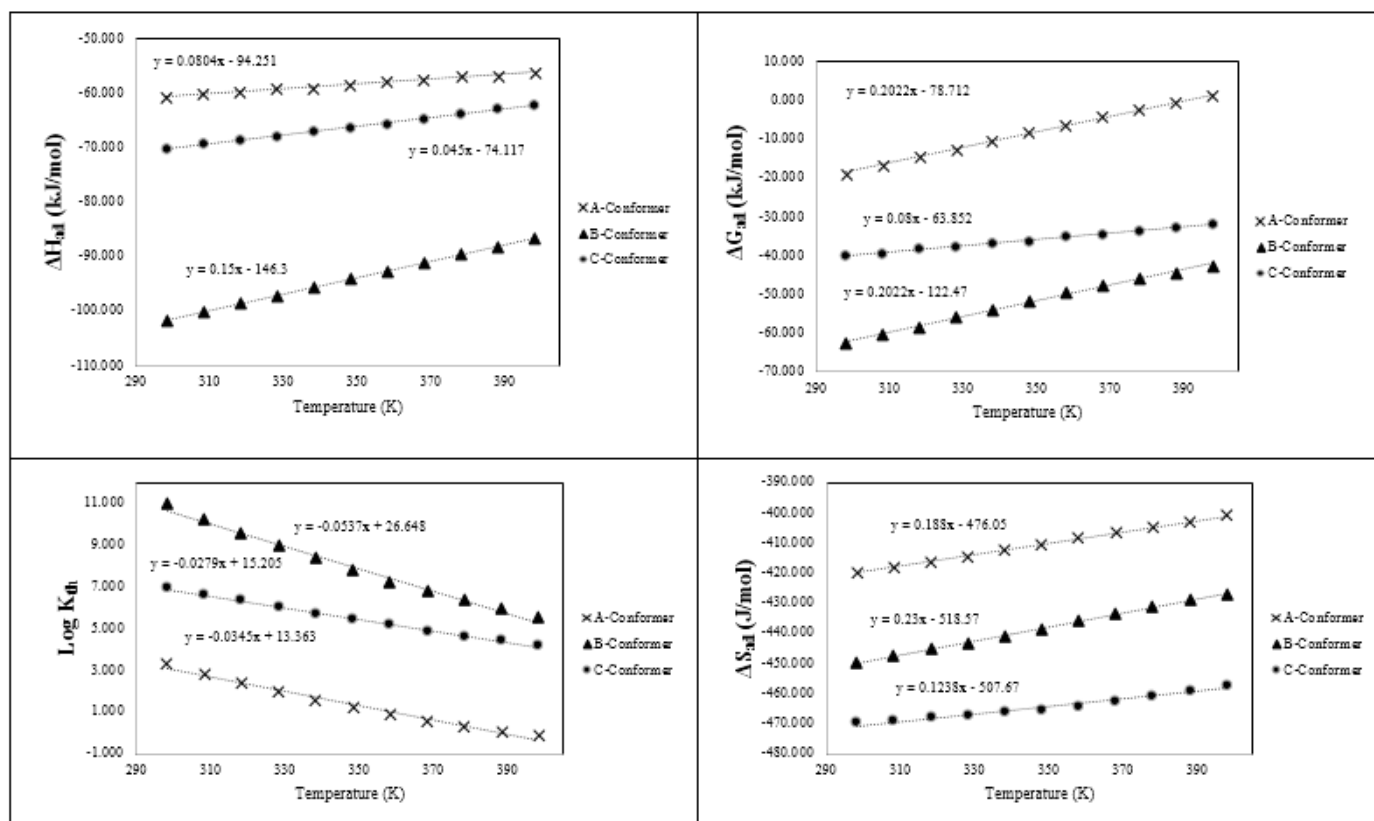


Figure 3. Thermodynamic parameters of NA adsorption process including ΔH_{ad} , ΔG_{ad} , ΔS_{ad} , and the logarithm of K_{th} in the temperature 298-398 K at 10° intervals

Table 2. The calculated FMO parameters for NA, C₂₀ and their complexes

NO	E_{HOMO} (eV)	E_{LUMO} (eV)	E_g (eV)	% ΔE_g	η (eV)	μ (eV)	ω (eV)	ΔN_{max} (eV)
NA	-5.821	5.066	10.887		5.443	-0.377	0.013	0.069
C20	-5.060	-3.110	1.950	---	0.975	-4.085	8.558	4.190
A-Conformer	-4.100	3.670	7.770	298.462	3.885	-0.215	0.006	0.055
B-Conformer	-4.580	3.160	7.740	296.923	3.870	-0.710	0.065	0.183
C-Conformer	-4.230	3.500	7.730	296.410	3.865	-0.365	0.017	0.094

Conclusion

This study used density functional theory computations to examine NA adsorption on the surface of fullerene (C_{20}). The negative values for E_{ad} , ΔG_{ad} , and ΔH_{ad} , as well as little values for K_{th} , showed that the NA interaction with fullerene was experimentally possible, exothermic, spontaneous, and reversible. The NBO results showed that NA and C_{20} did not form any chemical bond; hence, according to a physisorption adsorption process. The computed FMO parameters revealed that whereas C_{20} bandgap increased by +298.462% during the adsorption process. Because of the sharp variation of electrical conductivity during the adsorption process, it is clear that C_{20} makes a great sensing material for the development of cutting-edge electrochemical sensors for NA measurement. In this respect, the performance of the fullerene (C_{20}) as an adsorbent and sensing material for the removal and detection of NA is recommended to be evaluated by analytical chemist.

References:

- [1] L. Tahrani, L. Soufi, I. Mehri, A. Najjari, A. Hassan, J. Van Loco, H.B. Mansour, *Microb. Pathog.*, 89, 54-61 (2015).
- [2] Q. Wu, Z. Li, H. Hong, *Appl. Clay. Sci.*, 74, 66-73 (2013).
- [3] P.M. Torre, Y. Enobakhare, G. Torrado, S. Torrado, *Biomaterials*, 24(8), 1499-1506 (2003).
- [4] A.Y.C. Lin, T.H. Yu, C.F. Lin, *Chemosphere.*, 74(1),131-141 (2008).
- [5] F. Tamtam, F. Van Oort, B. Le Bot, T. Dinh, S. Mompelat, M. Chevreuil, M. Thiry, *Sci.Total. Environ.*, 409(3), 540-547 (2011).
- [6] A.J. Watkinson, E.J. Murby, D.W. Kolpin, S.D. Costanzo, *Sci. Total. Environ.*, 407(8), 2711-2723 (2009).
- [7] R.E. Morrissey, S. Eustis, J.K. Haseman, J. Huff, J.R. Bucher, *Drug.Chem.Toxicol.*, 14(1-2), 45-66 (1991).
- [8] A. Pollice, G. Laera, D. Cassano, S. Diomede, A. Pinto, A. Lopez, G. Mascolo, *J.Hazard. Mater.*, 203, 46-52 (2012).
- [9] K.J. Choi, S.G. Kim, S.H. Kim, *Environ.Technol.* 29(3), 333-342 (2008).

- [10] K.A. Robberson, A.B. Waghe, D.A. Sabatini, E.C. Butler, *Chemosphere.*, 63(6), 934-941 (2006).
- [11] I. Kim, N. Yamashita, H. Tanaka, *J. Hazard. Mater.*, 166(2-3), 1134-1140 (2009).
- [12] G. Roohi, G. Mahmoodi, H. Khoddam, *BMC Health. Serv. Res.*, 20(1), 1-9 (2020).
- [13] J. Beheshtian, A.A. Peyghan, Z. Bagheri, *Sens. Actuators B Chem.*, 171, 846-852 (2012).
- [14] S. Hussain, R. Hussain, M.Y. Mehboob, S.A.S. Chatha, A.I. Hussain, A. Umar, K. Ayub, *ACS omega.*, 5(13), 7641-7650 (2020).
- [15] S. Majedi, H.G. Rauf, M. Boustanbakhsh, *Chem. Rev. Lett.*, 2(4), 176-186 (2019).
- [16] R. Moladoust, *Chem. Rev. Lett.* 2(4), 151-156 (2019).
- [17] Nanotube Modeler *J. Crystal. Soft.*, 2014 software.
- [18] R. Dennington, T.A. Keith, J.M. Millam, Semichem Inc., Shawnee Mission, KS, GaussView, Version 6.1, 2016.
- [19] M.J. Frisch, G.W. Trucks, H.B. Schlegel, G.E. Scuseria, M.A. Robb, J.R. Cheeseman, G. Scalmani, V. Barone, G.A. Petersson, H. Nakatsuji, X. Li, M. Caricato, A.V. Marenich, J. Bloino, B.G. Janesko, R. Gomperts, B. Mennucci, H.P. Hratchian, J.V. Ortiz, A.F. Izmaylov, J.L. Sonnenberg, D. Williams-Young, F. Ding, F. Lipparini, F. Egidi, J. Goings, B. Peng, A. Petrone, T. Henderson, D. Ranasinghe, V.G. Zakrzewski, J. Gao, N. Rega, G. Zheng, W. Liang, M. Hada, M. Ehara, K. Toyota, R. Fukuda, J. Hasegawa, M. Ishida, T. Nakajima, Y. Honda, O. Kitao, H. Nakai, T. Vreven, K. Throssell, J.A. Montgomery, F. Ogliaro, M.J. Bearpark, J.J. Heyd, E.N. Brothers, K.N. Kudin, V.N. Staroverov, T.A. Keith, R. Kobayashi, J. Normand, K. Raghavachari, A.P. Rendell, J.C. Burant, S.S. Iyengar, J. Tomasi, M. Cossi, J.M. Millam, M. Klene, C. Adamo, R. Cammi, J.W. Ochterski, R.L. Martin, K. Morokuma, O. Farkas, J.B. Foresman, D.J. Fox, Gaussian, Inc., Wallingford CT, Gaussian 16, Revision C.01 (2016).
- [20] N.M. O'boyle, A.L. Tenderholt, K.M. Langner, *J. Comput. Chem.*, 29(5), 839-845 (2008).
- [21] M.R. Jalali Sarvestani, R. Ahmadi, *J. Phys. Theor. Chem.*, 15(1 (Spring and Summer 2018) 1 and 2): 15-25 (2018).
- [22] R. Ahmadi, M.R. Jalali Sarvestani, *J. Phys. Chem. B.*, 14, 198-208 (2020).
- [23] M.J. Jalali Sarvestani, R. Ahmadi, *Asian J. Nanosci. Mater.*, 3, 103-114 (2020).
- [24] M.R. Jalali Sarvestani, M. Gholizadeh Arashti, B. Mohaseb, *Int. J. New. Chem.*, 7(2), 87-100 (2020).

- [25] M.R. Jalali Sarvestani, R. Ahmadi, *Int. J. New. Chem.*, 4(4), 101-110 (2017).
- [26] M.J. Jalali Sarvestani, R. Ahmadi, *Chem. Methodol.*, 4, 40-54 (2020).
- [27] S. Majedi, F. Behmagham, M. Vakili, *J. Chem. Lett.*, 1(1), 19-24 (2020).
- [28] H. Ghafur Rauf, S. Majedi, E. Abdulkareem Mahmood, M. Sofi, *Chem. Rev. Lett.*, 2(3), 140-150 (2019).
- [29] R.A. Mohammed, U. Adamu, U. Sani, S.A. Gideon, A. Yakub, *Chem. Rev. Lett.*, 2(3), 107-117 (2019).
- [30] S. Majedi, H.G. Rauf, M. Boustanbakhsh, *Chem. Rev. Lett.*, 2(4), 176-186 (2019).
- [31] L. Hajiaghababaei, A.S. Shahvelayati, S.A. Aghili, *Anal. Bioanal. Electrochem.*, 7, 91-104 (2015).
- [32] S.S. Uroomiye, *Int. J. New. Chem.*, 6(3), 156-162 (2019).
- [33] A.S. Shahvelayati, I. Yavari, A.S. Delbari, *Chin. Chem. Lett.*, 25(1), 119-122 (2014).
- [34] M. R. Jalali Sarvestani, R. Ahmadi, *Journal of Physical & Theoretical Chemistry*, 15, 15-25 (2018).

HOW TO CITE THIS ARTICLE

Saeid Abrahi Vahed, Fatemeh Hemmati Tirabadi, “**A DFT Investigation on Fullerene (C₂₀) Interaction with Nalidixic Acid**” *International Journal of New Chemistry.*, 2022; 9(4), 393-404. DOI: 10.22034/ijnc.2022.706461